*H. C. Lim et al.*

# Diffusion and Kinetic-Controlled Electrochemical Reactions for Improving the Performance of Solution-based Electrochemiluminescence Devices

**Hong Chul Lim,[†,‡] Ji-Eun Park,[‡] Jong-In Hong,[†,*] and Ik-Soo Shin[‡,*]**

[†]*Department of Chemistry, Seoul National University, Seoul 08826, Republic of Korea.*
*E-mail: jihong@snu.ac.kr*
[‡]*Department of Chemistry, Soongsil University, Seoul 369, Republic of Korea. *E-mail: extant@ssu.ac.kr*

Electrochemiluminescence (ECL) refers to the generation of light at an excited state owing to an electron transfer reaction between the electrochemically generated species located around the electrode.[1–3] The ECL controlled by varying the potential has attracted attention for application in various fields, such as chemical analysis,[4] immunoassay,[5] and optoelectronic devices.[6] Among them, ECL devices (ECLDs) have recently been considered as promising next-generation displays due to their low energy consumption, simple fabrication process, and ability to function in direct current (DC) and alternating current (AC).[7–9] Most ECLDs have a single active layer, in which the ECL luminophore and electrolyte are mixed between two electrodes, acting as the anode and the cathode in a sandwich-type ECLD.[9,10] Thus, the working mechanism of ECLDs differs from those of conventional light-emitting diodes (LEDs).[7,11,12] This is due to the electrochemical system driven by the mass transfer of the mobile counter ions and luminophore present in the active layer.[10,11] When external force such as current or voltage is applied to the ECLDs, the electrolyte ions acting as the mobile counter ions is redistributed to each electrode, after which the electrochemical double layers (EDLs) form at the electrode/active layer interface, leading to the generating of a high electric field.[11,13] As a result, the electron transfer reaction between the electrode and the ECL luminophore occurs effectively, and an electric circuit, through which a faradaic current flows, is formed.[14,15] Consequently, the redox species encounter each other in the ECLDs to form an excited state through electron exchange, followed by a self-terminating ECL.[16,17] The ECL is affected both by the electron transfer rate ($k_o$) between the ECL luminophore and electrode and by the diffusion-limited reaction associated with the mass transfer of the ECL luminophore. These factors are determined by the operational method, and the type and concentration of the electrolyte.[9,15] Although several studies related to this subject have been reported, the dynamics of the electrochemical reactions involving the $k_o$ and the diffusion-limited reactions in ECLDs have not been properly elucidated.

This letter describes the kinetics of the electrochemical reactions in ECLDs under various electrolyte concentration and pulsed-voltage operating conditions. For the purpose of this study, self-terminating sandwich-type ECLDs were fabricated. Indium tin oxide (ITO) was employed as the electrode; bis(2-phenylquinoline) iridium (III) picolinic acid ((pq)$_2$Ir(pico)) and lithium perchlorate (LiClO$_4$) were used as the ECL luminophore and electrolyte, respectively. The ECLDs were operated under a pulsed-voltage-driven mode with various

frequencies (from 0.1 Hz to 100 Hz). We observed that the high concentration of the electrolyte interfered with the mass transfer of (pq)$_2$Ir(pico), thereby affecting the ECL intensity. In addition, the imperfection of the EDLs formed at the electrode/active layer interface under high frequencies reduced the effective potential drop, resulting in the suppression of the ECL by the $k_o$. Conversely, the ECL was observed upon the occurrence of the diffusion-limited reactions at low frequencies because most of the neutral (pq)$_2$Ir(pico) species around the electrode were consumed. Furthermore, the ECL intensity and continuity were dramatically improved with the pulsed alternating-voltage rather than the DC pulsed voltage and constant voltage.

The electrochemically stable (pq)$_2$Ir(pico) acid with a high ECL quantum yield was used as the ECL luminophore.[9,16] As the working mechanism of ECLDs is similar to that of bulk electrolysis in electrolytic cells, the electrolyte is a critical factor influencing the performance of ECLDs.[9] The electrolyte affects the formation of EDLs at the electrode/active layer interface, whereby an effective potential drop occurs.[9,18] Consequently, the electron transfer is facilitated by the outer-sphere mechanism between (pq)$_2$Ir(pico) and the electrode. Thereafter, the ECL phenomenon occurs effectively, owing to the electron exchange of the redox species.[19] However, the viscosity of the active layer is increased by increasing the electrolyte concentration so that the association of the mass transfer with the diffusion/migration of (pq)$_2$Ir(pico) is hindered, which decreases the brightness of the ECLDs.[20,21] To investigate the correlation between the mass transfer of (pq)$_2$Ir(pico) and the electrolyte concentration, cyclic voltammetry (CV) experiments were performed using a Pt ultramicroelectrode (UME, radius 25 μm) for measuring the diffusion coefficient ($D_o$) of (pq)$_2$Ir(pico). The electrochemical cell consists of three electrodes (a reference electrode (Ag/Ag$^+$ 0.01 M), a counter electrode (Pt), and a working electrode (Pt UME)) immersed in a propylene carbonate solvent containing 0.1 mM (pq)$_2$Ir(pico) with various concentrations of LiClO$_4$ as the electrolyte (from 50 to 700 mM). The $D_o$ values of (pq)$_2$Ir(pico) were derived using the Randles−Sevcik equation[22]:

$$I_{lim} = 4nFrC^*D_o \qquad (1)$$

where $I_{lim}$ is the limiting current (A), $n$ is the electron stoichiometry, $C^*$ is the (pq)$_2$Ir(pico) concentration (M), $D_o$ is the diffusion coefficient (cm$^2$/s), and $r$ is the electrode radius. The $D_o$ values of (pq)$_2$Ir(pico) according to the LiClO$_4$ concentration are depicted in

Figure 1(a) and summarized in Table S1 (Supporting Information). The decrease in the $D_o$ values of (pq)$_2$Ir(pico) with increasing LiClO$_4$ concentration indicates that the diffusion of the (pq)$_2$Ir(pico) was affected by the viscosity of the media with high LiClO$_4$ concentration, resulting in the reduced limiting current of (pq)$_2$Ir(pico).[21,23] This implies that the amount of (pq)$_2$Ir(pico) available for the redox reaction with the working electrode was reduced due to the sluggish diffusion of (pq)$_2$Ir(pico). The kinetic process of (pq)$_2$Ir(pico) in the sandwich-type ECLDs was studied by electrochemical impedance spectroscopy (EIS). The schematic diagram of the fabricated ECLD is shown in Figure S2. The Nyquist plots of the ECLDs exhibited a decreasing linear slope of the straight line in the low-frequency region with increasing applied voltage, as shown in Figure 2(b). A semicircle was observed in the devices with a bias of 2.4 V. Although the magnitude of the applied voltage (2.4 V) was less than the activation energy of the (pq)$_2$Ir(pico) redox reaction estimated from the potential difference between the oxidation ($E^o_{ox}$) and reduction ($E^o_{re}$) peak potentials, the internal electric field formed in the devices was higher than the triplet state of (pq)$_2$Ir(pico) ($E_T$ = 2.34 eV).[24] Thus, electrochemical redox reactions occurred through the electrode transfer reaction between (pq)$_2$Ir(pico) and the respective ITO electrodes, resulting in the generation of radical cations and anions at each ITO electrode.[12,16] The resistances of the solution were similar under the given LiClO$_4$ concentrations, as shown in Figure 1(c). Considering these results, Figure 1(d) shows the anticipated equivalent circuit of the ECLDs. $R_s$ and $C$ represent the device resistance and capacitance, respectively. $R_p$ and $C_{dl}$ indicate the resistance and capacitance of the electrical double layer at the interface between the ITO electrode and the active layer, respectively. $Z_w$ is the Warburg impedance involving the mass transfer of (pq)$_2$Ir(pico).[25]

Based on the results of the CV and EIS experiments, the ECL reactions in the ECLDs were investigated with a DC pulsed voltage of 2.5 V. The pulse driven method involves a square wave condition having a 50% duty cycle, which comprises of an active period with an applied voltage of 2.5 V and a resting period without an applied voltage of 2.5 V.[26] Figure 2(a) shows the monitored integrated ECL intensity as a function of the LiClO$_4$ concentration with various frequencies ranging from 0.1 to 100 Hz. At a frequency of 1 Hz, the active and resting periods applied to the ECLDs were 0.5 s. The electrochemical reactions associated with the ECL intensity and continuity were influenced by the LiClO$_4$ concentration and the frequency condition applied to the ECLDs. The ECL intensity of the ECLDs increased with the LiClO$_4$ concentration until 300 mM. However, the ECL intensity decreased at LiClO$_4$ concentrations higher than 300 mM. This behavior was consistent with the $D_o$ values of (pq)$_2$Ir(pico) obtained from the CV experiments mentioned above. This is because the mass transfer of (pq)$_2$Ir(pico) interfered at a high LiClO$_4$ concentration and consequently lowered the degree of formation of redox species. Eventually, the amount of (pq)$_2$Ir(pico)* species in the excited state, which could generate ECL, was lowered. Note that the ECL intensity appeared to depend on the applied frequency conditions, as shown in Figure 2(a). The lower the frequency applied to the ECLDs, the higher the ECL intensity. These results were attributed to the difference in the effective potential drop formed at the ITO/active layer interface depending on the frequency applied to the ECLDs.[9,10] In Figure 2(b), although the measured potential difference referring to the internal electric field in the ECLDs may not be the actual value, the effective potential was reduced as the frequency of the DC pulsed voltage increased. These results indicated that the effective potential was not achieved

completely at high frequencies due to the ionic motions that could not be traced within the active short transient time period. This leads to the incomplete formation of the EDLs at the ITO/active layer interface. Thus, the ECL intensity is relatively enhanced at a low frequency compared to the case at a high frequency due to the effectively formed redox species of (pq)$_2$Ir(pico). Another interesting result was the continuous ECL emission observed at frequencies above 10 Hz, as shown in Figure 3(a), which was attributed to the capacitance effect as well as the diffusion-limited reaction of the ECL transition.[11,27] Moreover, it was associated with the equivalent circuit of the ECLDs, as depicted in Figure 1(d). When operating the ECLDs with a DC pulsed voltage at 10 Hz (50% duty cycle, the active and resting period are 50 ms), only a part of (pq)$_2$Ir(pico) induced electrochemical reactions with the ITO electrode during the short active period due to the relatively low effective potential drop. Therefore, most of the neutral (pq)$_2$Ir(pico) species that did not participate in the redox reactions are located around both the ITO electrodes. In addition, the capacitance effect owing to the EDLs generates instantaneous negative potential in the ECLDs at the resting period.[27,28] This confirms that a negative current flowed during the resting period, as shown in Figure 3(b) and Figure S3. These results indicate that the neutral (pq)$_2$Ir(pico) was reduced by the electron transfer with the ITO electrode during the resting period. In general, when (pq)$_2$Ir(pico) is oxidized, the value of the current is represented by a "+" sign. The sign of the reduction current is the reverse: "−."[16,17] The excited state of (pq)$_2$Ir(pico)* was generated by a followed electron exchange between the redox species, which diffused/migrated to the opposite electrode or located redox species around the electrodes.[1,16] Consequently, the continuous ECL emission with low ECL intensity occurred at frequencies above 10 Hz. Conversely, discontinuous ECL emission was observed below 0.1 Hz, having an active and resting period of 5 s, as depicted in Figure 3(a). In other words, (pq)$_2$Ir(pico) is mostly oxidized/reduced near each electrode during the active period. Subsequently, the redox species that diffused to the opposite electrode undergo electron exchange between them to form the (pq)$_2$Ir(pico) excited state. Under this condition, the concentration of (pq)$_2$Ir(pico)* was depleted because the redox species of (pq)$_2$Ir(pico) were not replenished around each electrode. As a result, the ECL intensity decreased during the resting period.

Based on these experimental results, we anticipated that a continuous and high ECL intensity would be observed when a voltage with an alternating polarity is applied to the ECLDs. The electron exchange of the redox species occurs at the same electrode, thereby allowing the effective formation of the (pq)$_2$Ir(pico)* species, making the ECL emission promptly achievable with a high ECL intensity.[9,29] Since the standard alternating frequency is 50 or 60 Hz, the experimental condition was set such that a square-wave pulsed alternating voltage with a peak-to-peak voltage ($V_{pp}$) of 5 V (60 Hz, 50% duty cycle) was applied on the ECLDs. The $V_{pp}$ of 5 V means ±2.5 V was applied at the same electrode. Interestingly, the pulsed alternating-voltage driving method exhibited different ECL tendencies compared to the DC pulsed voltage and constant voltage driving methods. The ECL intensity and continuity were improved in the pulsed alternating-voltage-driven mode, as shown in Figure 4. Furthermore, the ECL intensity decreased dramatically under the constant-voltage-driven mode, compared to the case under other modes. We attributed the improvement in the ECL intensity and continuity to the joint influences of two factors. Firstly, the given frequency (60 Hz) provides time for the most kinetically favored redox reactions with an effective potential drop at the electrode/active layer
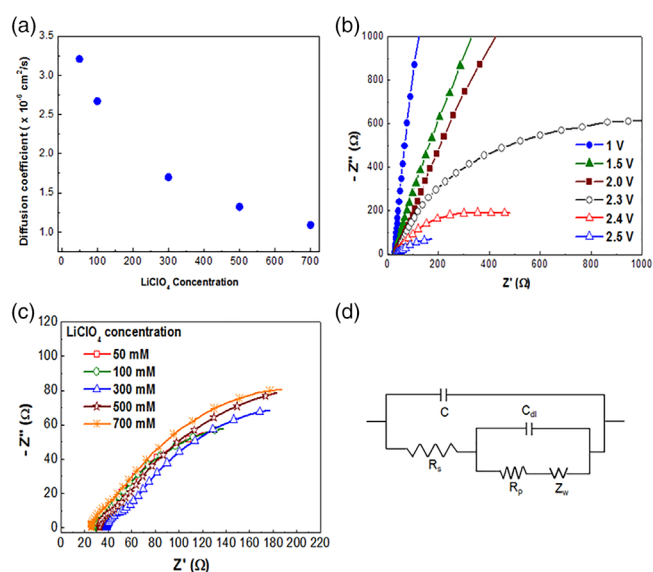
**Figure 1.** (a) Steady-state current as a function of the LiClO₄ concentration with 0.1 mM (pq)₂Ir(pico) and a 25 μm Pt microdisk electrode. The Nyquist plots of the AC impedance for the ECLDs (b) with various applied biases with 14 mM (pq)₂Ir(pico) and 300 mM LiClO₄; (c) with various LiClO₄ concentrations at 2.5 V, and (d) the anticipated equivalent circuit of the ECLDs.

interface. Secondly, the excited state of (pq)₂Ir(pico)* is formed around both electrodes and in the bulk layer so that the concentration of the neutral (pq)₂Ir(pico) species is replenished near both electrodes.[30] These results suggest that the electrochemical reactions involving ECL may occur via different kinetic pathways according to the driven mode.
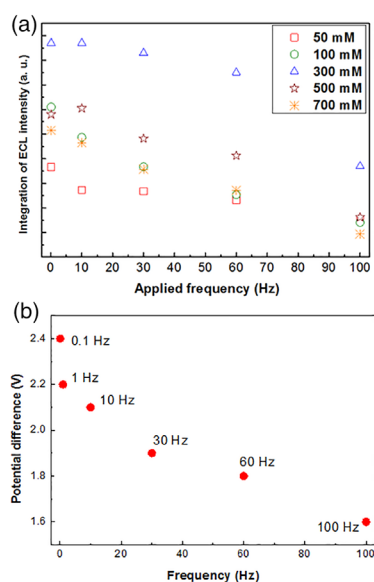


**Figure 2.** Plot of the integrated ECL intensity on the DC pulsed voltage at 2.5 V with 50% duty cycle as a function of the frequency and various LiClO₄ concentrations (from 50 to 700 mM), and (b) potential difference between the electrode and the active layer at DC pulsed voltage with various operational frequencies in ECLDs with 300 mM LiClO₄.
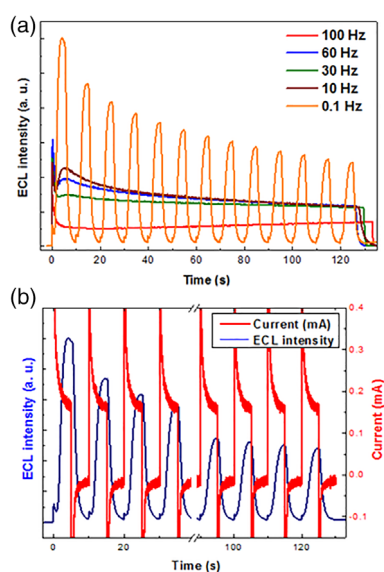


**Figure 3.** (a) Temporal ECL intensity of the DC pulsed voltage with various operational frequencies from 0.1 to 100 Hz, and the (b) temporal ECL intensity and redox reaction current at 0.1 Hz. The sandwich-type ECLDs comprised of 14 mM (pq)₂Ir(pico) and 300 mM LiClO₄.

In summary, the electrochemical reactions were investigated including the mass transfer and kinetics in ECLDs. Both the LiClO₄ concentration and the operating methods in the ECLDs influenced the electrochemical reactions of (pq)₂Ir(pico), but the electron transfer between (pq)₂Ir(pico) and the electrode was effectively induced by the EDLs formed by LiClO₄ at the electrode/active layer interface. In addition, the diffusion rate of (pq)₂Ir(pico) was reduced at a high LiClO₄ concentration, which consequently reduced the ECL intensity. When applying the pulsed alternating-voltage driving conditions to the ECLDs, the ECL intensity and continuity were improved compared with those obtained by the DC pulsed and constant voltage modes. These results indicate the importance of controlling the rate of electrochemical reactions to achieve high ECL
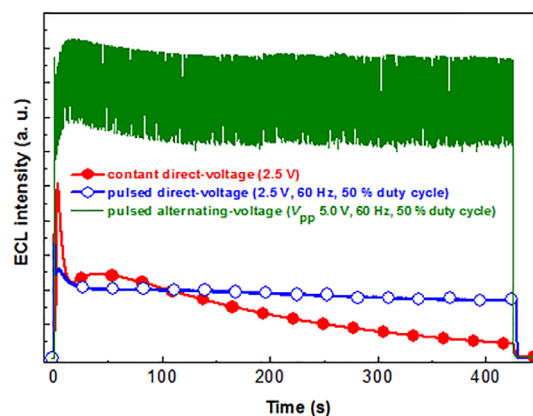


**Figure 4.** Comparison of the temporal ECL intensity with various operating driven-mode. (line: pulsed alternating-voltage mode ($V_{pp}$ 5.0 V, 60 Hz, and 50% duty cycle), line with open symbol: DC pulsed voltage mode (2.5 V, 60 Hz, and 50% duty cycle), and line with closed symbol: constant voltage mode (2.5 V).

brightness in ECLDs. The electrochemical investigation suggested in this study is expected to provide useful information for the development of high performance ECLDs.

## Experimental

**Reagents and Instruments.** All the chemical reagents used in this study are commercially available and were used without further purification. Lithium perchlorate (LiClO$_4$) and propylene carbonate (PC) were purchased from Sigma-Aldrich (St. Louis, MO, USA). A scanning electron microscope (SEM) was used (SEM, Hitachi S-4300, Tokyo, Japan) for confirming the space between the ITO electrodes of the ECLDs.

**Fabrication of ECLDs.** A sandwiched device configuration was employed: ITO/active layer/ITO. The ITO electrode (10 Ω/sq., SNI Inc., Seongnam, South Korea) on glass substrate was cleaned by sequential ultrasonication in deionized water (15 min) and isopropyl alcohol (15 min), followed by drying of the ITO electrodes in an oven overnight (120 °C). One of the two ITO electrodes had three holes with 1 mm diameters for injecting an electroactive solvent. Thermal tape (Solaronix Co., Aubonne, Switzerland) was used to attach the two ITO electrodes and to prevent the solvent leakage. The distance between the two ITO electrodes was 60 μm. The resulting sandwich-type substrates were attached by heating at 80 °C for 10 min on a hot plate. Subsequently, the prepared solution, by blending 14 mM (pq)$_2$Ir(pico) with various LiClO$_4$ concentrations (from 50 to 700 mM) in PC, was injected through the hole. Finally, the holes were sealed using a hot-melt polymer film with a cover glass (0.1 mm thick). The emission area of the ECLDs was $1.5 \times 1.5$ cm$^2$.

**Characterization.** Electrochemical impedance spectroscopy, cyclic voltammetry, and light emission of the ECLDs were performed using a CH Instruments 650B Electrochemical Analyzer (CH Instruments Ins., Austin, TX). The ECL emissions were recorded using a photomultiplier tube mode (PMT, Hamamatsu photonics H6780, Shizuoka, Japan). The fabricated ECLDs were mounted directly on the PMT to measure the ECL intensity.

**Supporting Information.** Additional supporting information may be found online in the Supporting Information section at the end of the article.

## References

1. K. S. V. Santhanam, A. J. Bard, *J. Am. Chem. Soc.* **1965**, *87*, 139.

2. L. R. Faulkner, A. J. Bard, *J. Am. Chem. Soc.* **1968**, *90*, 6284.

3. L. R. Faulkner, A. J. Bard, *Electrogenerated Chemiluminescence*, Vol. 10, Marcel Dekker, New York, **1977**, p. 1.

4. I.–S. Shin, S. W. Bae, H. Kim, J.–I. Hong, *Anal. Chem.* **2010**, *82*, 8259.

5. W. Zhan, A. J. Bard, *Anal. Chem.* **2007**, *79*, 459.

6. G. H. Brilmyer, A. J. Bard, *J. Electrochem. Soc.* **1980**, *127*, 104.

7. D. Laser, A. J. Bard, *J. Electrochem. Soc.* **1975**, *122*, 632.

8. Q. Pei, G. Yu, C. Zhang, Y. Yang, A. J. Heeger, *Science* **1995**, *269*, 1086.

9. E.–S. Ko, J. I. Lee, H. C. Lim, J.–E. Park, S. H. Kong, M. S. Kang, I.–S. Shin, *ACS Photonics* **2018**, *5*, 3723.

10. T. Nobeshima, M. Nakakomi, K. Nakamura, N. Kobayashi, *Adv. Optical Mater.* **2013**, *1*, 144.

11. S. van Reenen, P. Matyba, A. Dzwilewski, R. A. J. Janssen, L. Edman, M. A. Kemerink, *J. Am. Chem. Soc.* **2010**, *132*, 13776.

12. Y. Li, J. Gao, G. Yu, Y. Cao, A. J. Heerger, *Chem. Phys. Lett.* **1998**, *287*, 83.

13. S. A. Cruser, A. J. Bard, *J. Am. Chem. Soc.* **1969**, *91*, 267.

14. C. Mavré, K.–F. Chow, E. Sheridan, B.–Y. Chang, J. A. Crooks, R. M. Crooks, *Anal. Chem.* **2009**, *8*, 6218.

15. J. Zhang, F. Zhao, T. Abe, M. Kaneko, *Electrochim. Acta* **1999**, *45*, 399.

16. I.–S. Shin, J. I. Kim, T.–H. Kwon, J.–I. Hong, J.–K. Lee, H. Kim, *J. Phys. Chem. C* **2007**, *111*, 2280.

17. R. Ishimatsu, S. Matsunami, T. Kasahara, J. Mizuno, T. Edura, C. Adachi, K. Nakano, T. Imato, *Angew. Chem. Int. Ed.* **2014**, *53*, 6993.

18. F. Croce, G. B. Appetecchi, P. Mustarelli, E. Quartarone, C. Tomasi, E. Cazzanelli, *Electrochim. Acta* **1998**, *43*, 144.

19. M. Pikulski, W. Gorski, *Anal. Chem.* **2000**, *72*, 2696.

20. C. Beriet, D. Pletcher, *J. Electroanal. Chem.* **1993**, *361*, 93.

21. K. M. Maness, J. E. Bartelt, R. M. Wightman, *J. Phys. Chem.* **1994**, *98*, 3993.

22. U. K. Sur, A. Dhason, V. Lakshminarayanan, *J. Chem. Educ.* **2012**, *89*, 168.

23. H. P. Chen, J. W. Fergus, B. Z. Jang, *J. Electrochem. Soc.* **2000**, *147*, 399.

24. R. S. Nicholson, I. Shain, *Anal. Chem.* **1964**, *36*, 706.

25. S.–C. Chang, Y. Yang, F. Wudl, G. He, Y. Li, *J. Phys. Chem. B* **2001**, *105*, 11419.

26. T. Nobeshima, T. Morimoto, K. Nakamura, N. Kobayashi, *J. Mater. Chem.* **2010**, *20*, 10630.

27. S. Pastore, F. Magno, M. M. Collinson, R. M. Wightman, *J. Electroanal. Chem.* **1995**, *397*, 19.

28. K.–C. Tsay, L. Zhang, J. Zhang, *Electrochim. Acta* **2012**, *60*, 428.

29. N. M. Shavaleev, R. Scopelliti, M. Grätzel, M. K. Nazeeruddin, A. Pertegás, C. Roldán-Carmona, D. Tordera, H. J. Bolink, *J. Mater. Chem. C* **2013**, *1*, 2241.

30. S. Shin, Y. S. Park, S. Cho, I. You, I. S. Kang, H. C. Moon, U. Jeong, *Chem. Sci.* **2018**, *9*, 2480.